Calcium-activated chloride current amplifies the response to urine in mouse vomeronasal sensory neurons

Chun Yang and Rona J. Delay

Department of Biology, University of Vermont, Burlington, VT 05405

The vomeronasal organ (VNO) is an odor detection system that mediates many pheromone-sensitive behaviors. Vomeronasal sensory neurons (VSNs), located in the VNO, are the initial site of interaction with odors/pheromones. However, how an individual VSN transduces chemical signals into electrical signals is still unresolved. Here, we show that a Ca^{2+}-activated Cl^- current contributes ~80% of the response to urine in mouse VSNs. Using perforated patch clamp recordings with gramicidin, which leaves intracellular chloride undisrupted, we found that the urine-induced inward current (V_{hold} = −80 mV) was decreased in the presence of chloride channel blockers. This was confirmed using whole cell recordings and altering extracellular chloride to shift the reversal potential. Further, the urine-induced currents were eliminated when both extracellular Ca^{2+} and Na^+ were removed. Using inside-out patches from dendritic tips, we recorded Ca^{2+}-activated Cl^- channel activity. Several candidates for this Ca^{2+}-activated Cl^- channel were detected in VNO by reverse transcription–polymerase chain reaction. In addition, a chloride cotransporter, Na^+-K^+-$2Cl^-$ isoform 1, was detected and found to mediate much of the chloride accumulation in VSNs. Collectively, our data demonstrate that chloride acts as a major amplifier for signal transduction in mouse VSNs. This amplification would increase the responsiveness to pheromones or odorants.

The Journal of General Physiology

INTRODUCTION

Most mammals have four olfactory systems, the main olfactory epithelium (MOE), the vomeronasal organ (VNO), the septal organ, and the Grueneberg ganglion. MOE responds to general odorants and some pheromones. Most of these responses are mediated by the cAMP pathway, although other pathways are thought to mediate some responses (Schild and Restrepo, 1998; Zufall and Leinders-Zufall, 2007). For the odorants where the response is mediated by the cAMP pathway, activation of odorant receptors on the cilia leads to the increase of $[cAMP]_i$, which directly activates the CNG channels and leads to the influx of Na^+ and Ca^{2+} (Zufall et al., 1994; Kleene, 2008). The influx of Ca^{2+} activates Ca^{2+}-activated Cl^- channels, greatly amplifying the small inward current through the CNG channel (Kurahashi and Yau, 1993; Kleene, 1997). The septal organ appears to work similarly to MOE, and it is not clear what the role of the Grueneberg ganglion is (Breer et al., 2006).

However, the VNO responds to many pheromones and some odorants. In mammals, VNOs are paired tubular structures enclosed by a bony or cartilaginous capsule located next to the nasal septum with an opening to the nasal cavity through a narrow duct (Døving and Trotier, 1998; Keverne, 1999; Breer et al., 2006). Vomeronasal sensory neurons (VSNs) are bipolar cells located in the sensory epithelium of the VNO, each with a dendritic knob and microvilli exposed to chemicals in the lumen. Their axons project to the accessory olfactory bulb in the central nervous system (Døving and Trotier, 1998; Keverne, 1999). The receptors for pheromones or general odorants located at the microvillar membrane are also G protein ($G_{\alpha i}$ or $G_{\alpha o}$) –coupled proteins. After the binding of a pheromone/odorant, these GTP-bound G proteins activate phospholipase C, increasing diacylglycerol. Elevation of diacylglycerol leads to the opening of cation channels (e.g., transient receptor potential channel 2 [TRPC2] channel) and the influx of Na^+ and Ca^{2+} (Lucas et al., 2003). Further downstream activation of channels or enzymes has only recently been explored, focusing primarily on adaptation (Zhang et al., 2008; Spehr et al., 2009). If there is a downstream mechanism for amplifying the current carried by Na^+/Ca^{2+} as there is in olfactory sensory neurons (OSNs), then the signal-to-noise of pheromone/odorant detection for VSNs would be greatly increased.

To test for the possibility of Ca^{2+}-activated Cl^- channels amplifying the response of VSNs, we used a combination of chloride channel blockers and ion substitution. We determined that Cl^- carried most of the urine-induced

Correspondence to Rona J. Delay: rdelay@uvm.edu

Abbreviations used in this paper: Ano, anoctamin; Best, bestrophin; DIDS, 4,4'-diisothiocyanatostilbene-2,2'-disulfonic acid; KCC, potassium-chloride cotransporter; MOE, main olfactory epithelium; NKCC, sodium-potassium-chloride cotransporter; NKCC1, Na^+-K^+-$2Cl^-$ isoform 1; OSN, olfactory sensory neuron; RT, reverse transcription; TRPC2, transient receptor potential channel 2; VNO, vomeronasal organ; VSN, vomeronasal sensory neuron.

The Rockefeller University Press $30.00
J. Gen. Physiol. Vol. 135 No. 1 3–13
www.jgp.org/cgi/doi/10.1085/jgp.200910265

current in mouse VSNs. The chloride current that amplified urine responses appeared to be dependent on a Ca^{2+} influx. By using reverse transcription (RT)-PCR and immunocytochemistry, we detected the expression of a chloride cotransporter, Na^+-K^+-$2Cl^-$ isoform 1 (NKCC1) in VSNs. A specific blocker for sodium-potassium-chloride cotransporter (NKCC), bumetanide, significantly decreased the urine-induced inward current, suggesting a function for NKCC1 in chloride accumulation. In contrast, a blocker for potassium-chloride cotransporter (KCC), furosemide, which moves chloride out of the cell, had no effect on the urine-induced inward current. Moreover, Ca^{2+}-activated Cl^- channels were detected in inside-out patches from dendritic tips of VSNs. RT-PCR data suggest there are several possible candidates for this Ca^{2+}-activated Cl^- channel. Our data provide a mechanism for signal amplification in VSNs in response to pheromones/odorants. The accumulation of intracellular Cl^- by NKCC1 allows the amplification of the response to pheromones/odorants by the Ca^{2+}-activated Cl^- channels when the transduction pathway is activated.

MATERIALS AND METHODS

Preparation of isolated VSNs

All of the animals used in this study were maintained and euthanized in accordance with the University of Vermont Animal Care and Use Committee guidelines. 2–6-month-old C57BL/6 and BALB/c mice of were used for all experiments. These mice were maintained in open wire-topped cages on a 12-h light–12-h dark cycle with food and water available at all times. Mice were euthanized with CO_2 inhalation followed by cervical dislocation. The VNOs were dissected out, and the tissue from the VNOs was cut into small pieces and incubated in a divalent cation-free mouse saline solution (in mM: 140 NaCl, 10 HEPES, 10 glucose, and 5 KCl, pH 7.4) with 55 µg/ml papain for 15 min at room temperature. After filtration through a nylon mesh, the cells were kept in Ringer's (in mM: 138 NaCl, 10 HEPES, 10 glucose, 2 $MgCl_2$, 2 $CaCl_2$, and 5 KCl, pH 7.4) with 11 µg/ml leupeptin for 15 min, and then in Ringer's up to 4 h. The VSNs from both strains of mice did not show any difference in urine responses.

Urine collection

Urine was collected from both sexes of C57BL/6 and BALB/c mice by gently pressing on each abdomen. After pooling the urine from more than 30 mice, it was filtered with a 0.2-µm filter and frozen at −80°C. Before use, the urine mixture was diluted to 1:500 in Ringer's (pH 7.4). At this dilution, the urine has no influence on osmolarity.

Chemicals or drugs

All chemicals were purchased from Sigma-Aldrich unless stated otherwise. Stock solutions of niflumic acid, bumetanide, and furosemide were made in DMSO and stored at −80°C. Before use, these chemicals were diluted in Ringer's to the final concentration (300 µM for niflumic acid, 10 or 50 µM for bumetanide, and 100 µM for furosemide). DMSO alone (0.05–0.2%) had no effect on urine responses. The 4,4'-diisothiocyanatostilbene-2,2'-disulfonic acid (DIDS) solution (300 µM) was freshly made before each experiment.

Electrophysiology

Isolated VSNs were placed onto a recording chamber and viewed with an inverted microscope (TE2000S; Nikon).

Perforated patch clamp recordings. Gramicidin was used as a channel-forming agent. The pores formed by gramicidin allow the flow of Na^+ and K^+, but not Cl^-. Gramicidin was freshly dissolved in DMSO before each experiment, and then mixed with intracellular solution (in mM: 110 K-gluconate, 10 HEPES, 1 EGTA, 10 NaCl, 1 $MgCl_2$, 0.023 $CaCl_2$, and 30 KCl, pH 7.4) by sonication for 15 min. Electrodes with a resistance of 6–10 MΩ were filled with the intracellular solution in the tips and intracellular solution with 0.27 mg/ml gramicidin in the back. After a giga seal was established, it took 20 min to 1 h for complete perforation to occur. The success of complete perforation was evaluated by the peak of voltage-activated inward currents (within 10 ms of voltage stimuli) in voltage steps from −90 to +90 mV with 20-mV increments. Urine responses were recorded at a holding potential of −80 mV. Nominally zero (<< 10 nM) Ca^{2+} Ringer's was (in mM): 138 NaCl, 10 HEPES, 2 $MgCl_2$, 0.02 $CaCl_2$, 5 KCl, and 5 EGTA, pH 7.4, and 285 mmol/kg (glucose). Zero Ca^{2+}-zero Na^+ Ringer's was (in mM): 138 cholineCl, 10 HEPES, 2 $MgCl_2$, 0.02 $CaCl_2$, 5 KCl, and 5 EGTA, pH 7.4, and 285 mmol/kg (glucose).

Whole cell patch clamp. Electrodes with a resistance of 7–14 MΩ were filled with the following solution (in mM): 140 mM CsCl, 10 HEPES, 5 EGTA, 1 Mg-ATP, and 0.5 Mg-GTP, pH 7.4, and 285 mmol/kg (glucose). After giga seal (>1 GΩ) formation on the soma, suction was used to obtain the whole cell recording configuration. Low Na Ringer's contained (in mM): 118 cholineCl, 20 NaCl, 10 HEPES, 2 $MgCl_2$, 2 $CaCl_2$, and 5 KCl, pH 7.4, and 285 mmol/kg (glucose). Low Cl^- Ringer's contained (in mM): 111 Na-gluconate, 27 NaCl, 10 HEPES, 2 $MgCl_2$, 2 $CaCl_2$, and 5 KCl, pH 7.4, and 285 mmol/kg (glucose). Urine responses were recorded at voltage steps from −80 to +80 mV (20-mV increments) with 3 M KCl agar bridge or with Ag/AgCl ground wire in a separate but connected Ringer's-filled chamber.

Inside-out patches. We used membrane from dendritic tips of mouse VSNs using electrodes with a resistance of 10–18 MΩ. Channel activity was recorded in symmetric solution (in mM): 140 cholineCl, 10 HEPES, and 1 EGTA, pH 7.4, and 285 mmol/kg (glucose). Bath calcium concentrations were adjusted to 150 nM or 1 mM by adding $CaCl_2$. Free [Ca^{2+}] values were determined with Winmaxc 2.5 software.

In all the electrophysiological experiments, currents were recorded using Digidata 1322A, Multiclamp 700A, and pClamp 8.2 software programs (MDS Analytical Technologies). Data were Bessel filtered at 4 kHz with sampling intervals at 10 kHz. The single-channel data were further filtered at 30 Hz with the eight-pole Bessel filter for display purposes only. A Warner fast-step SF-77B perfusion system, which provides stimuli within 10–20 ms, was used to deliver stimuli. Some blockers were bath delivered using a gravity-fed bath perfusion system.

Electrophysiology data analysis

Clampex 8.2 software (MDS Analytical Technologies) was used to measure the amplitude of the urine-induced inward currents. In the figures, the amplitude of urine-induced inward currents in different testing solutions was normalized for each cell to that recorded in Ringer's. However, for the statistical analysis, we used the raw data. Histograms and box plots were used to determine if the data had a normal distribution and if the data contained any outliers. For data with a normal distribution and without any outliers, a paired *t* test or repeated measures one-way ANOVA with Bonferroni test was performed to check the statistical significance. Otherwise, Wilcoxon signed rank test or Friedman with Dunn test

was performed for statistical analysis. Minitab 15 or GraphPad (GraphPad Software, Inc.) was used for making the histograms, box plots, and statistical tests.

RT-PCR

Total RNA was extracted from dissected VNOs, treated with DNase I, and purified according to the manufacturer's instructions (kit no. 78765; Affymetrix). Two-step RT-PCR was performed to test the expression of target genes. cDNA was synthesized by using 1.25 µM oligo dT (Invitrogen), 0.15 µg of random primers (Invitrogen), and 200 U SuperScript III RT (Invitrogen) from ~2 µg of total RNA in a total volume of 20 µl. RNase OUT ribonuclease inhibitor (Invitrogen) was added to protect the RNA from degradation. PCR was done using 2 µl cDNA as templates and specific primers for target genes in a total volume of 50 µl. For a negative control, the same amount of RNA (~2 µg) was treated using the same method as that for cDNA synthesis but without any RT in the synthesis step. 2 µl of this negative control product was used as templates to ensure there was no DNA contamination. PCR cycles were as follows: 95°C 5 min; (95°C 1 min, specific annealing temperature 1 min, 72°C 1 min: 35 cycles); 72°C 10 min. *Nkcc1*: F-5′-CTATGCTCCGGTTCACGCAG-3′ and R-5′-GGACGCTCTGATGATTCCCAC-3′ (annealing temperature 60°C; product length, 1,061 bp; GenBank accession no. NM_009194); *anoctamin* (*Ano*) *1*: F-5′-TAAAGATTACCGGGAACCCC-3′ and R-5′-CTGCTCCTCACGCATAAACA-3′ (annealing temperature, 58°C; product length, 226 bp; GenBank accession no. NM_178642); and *Ano2*: F-5′-TCCTATAGCCACAACGGGAC-3′ and R-5′-CTTAAGCCAGTTCCCAGCAG-3′ (annealing temperature, 58°C; product length, 607 bp; GenBank accession no. NM_153589). Primers for the bestrophin (Best) family were the same as those used by Pifferi et al. (2006). PCR products were sequenced at Vermont Cancer Center DNA Analysis facility.

Immunocytochemistry

Isolated VSNs from four adult mice, prepared as described above, were used. Cells were plated onto concanavalin A–coated coverslips and fixed with 4% paraformaldehyde in 0.1 M of phosphate buffer, pH 7.4, for 90 min. After rinsing with buffer six times, the cells were incubated with the blocking solution (8% normal goat serum and 0.6% Triton X-100 in phosphate buffer saline, pH 7.4) for 1 h, and then with a specific rabbit anti–rat NKCC1 antibody (1:200) overnight. The NKCC1 antibody recognizes the cytoplasmic C terminus from rat NKCC1 (GenBank accession no. MP 113986.1; Alpha Diagnostic Intl. Inc.). The cells were washed several times after the primary antibody, and then incubated with goat anti–rabbit Rhodamine RedX-628 (1:500; Invitrogen) for 1 h. Cells treated the same as the experimental ones but without any primary antibody were used as the negative controls. Images for both experimental and control cells were taken and displayed at the same conditions and the same day with a Deltavision deconvolution microscope system at University of Vermont COBRE Imaging Facility. In brief, cells were viewed under an inverted microscope (IX70; Olympus). The images were taken by a photometrics coolsnap HQ camera (using interline Sony ICX285 CCD) with rhodamine filters (excitation wavelength, 541–569 nm; emission wavelength, 580–654 nm) at 0.1-s exposure. After deconvolution, images were displayed by SoftWoRx Explorer (Applied Precision) software.

RESULTS

Dilute urine-induced inward currents in isolated mouse VSNs

Urine has been reported to evoke a calcium influx and action potentials in VSNs (Zufall et al., 2002;

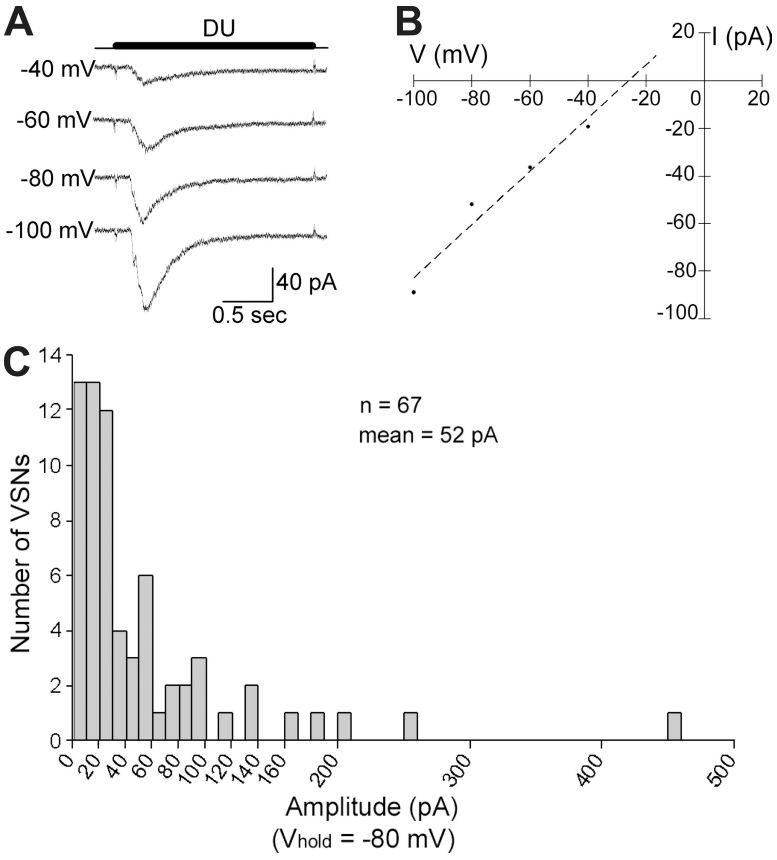

Figure 1. Isolated mouse VSNs responded to dilute urine. (A) Perforated patch clamp recordings from the soma showed inward currents induced by a 2-s application of urine at voltage steps from −100 to −40 mV (20-mV increments). The time for the urine application is shown by the dark line above current traces. DU, 1:500 dilute urine. (B) I-V plot for the urine response of the VSN shown in A. Dashed line shows the best-fit line ($y = 1.1183x$ plus 29.118; $R^2 = 0.9521$). (C) Summary of the peak amplitudes for urine-induced inward currents at V_{hold} = −80 mV for 67 urine-responsive VSNs (one to two cells per mouse).

Zhang et al., 2008), but the current response to urine without artificial changes in intracellular chloride has not been investigated. Thus, in the first series of experiments, we used the perforated patch clamp technique with gramicidin as the pore-forming agent to record the responses of isolated mouse VSNs to dilute urine (1:500). Gramicidin allows Na^+ and K^+ to pass, but not Cl^- nor any diffusible second messengers. The response to urine was measured at holding potentials from −100 to −40 mV. Each current trace was 5 s long with urine applied in the middle of each trace for 2 s (only part of 5-s traces are shown). In the majority of the cells tested (7 out of 10), urine induced inward currents at all of these holding potentials. For each holding potential, an inward current was elicited after 0.1–0.2 s of urine application, and then increased until it reached the peak at ∼0.3 s, after which the response decreased (Fig. 1 A). Due to possible involvement of potassium channels, especially large-conductance calcium-activated potassium channels, by downstream effects of the transduction pathway (Zhang et al., 2008), the actual reversal potential of the urine response was not determined. However, the peak of the urine-induced inward currents showed an apparent linear relationship to holding potentials from −100 to −40 mV. A best-fit line through the data points crossed the x axis near −25 mV (Fig. 1 B). The influx of cations through TRPC2 channels has a reversal potential close to 0 mV (Lucas et al., 2003). The negative reversal potential of urine responses could be explained by an involvement of an anion.

Because the peak of the inward current occurred within 0.5 s of urine application and the resting membrane potential of VSNs is between −50 and −75 mV (Shimazaki et al., 2006; Ukhanov et al., 2007), we decided to use a protocol with a 0.5-s urine application at a holding potential of −80 mV for the rest of the perforated patch clamp experiments. At −80 mV, ∼60% of VSNs (67 out of 111 cells; 92 animals) displayed urine-induced inward currents, most of which had peak amplitudes between −5 and −150 pA (Fig. 1 C). Thus, dilute urine, a complex mixture of ions, chemicals, and compounds, induced inward currents with various amplitudes in most VSNs at a holding potential of −80 mV.

Chloride current contributed to the urine response in native VSNs

To test if chloride was involved in the urine response in isolated VSNs, we applied two commonly used extracellular chloride channel blockers, 300 µM DIDS and 300 µM niflumic acid (Nilius and Droogmans, 2003; Hartzell et al., 2005), and tested their influence on urine-induced inward currents. These blockers alone did not evoke any response in VSNs (unpublished data). To control for adaptation caused by repetitive stimulation, urine applications were at least 2 min apart so each VSN had completely recovered before the next stimulus. As shown in Fig. 2 A, dilute urine induced an inward current (with a peak amplitude of −123 pA for this VSN). After a 2-min wash, the cell was incubated in 300 µM DIDS for 1 min before it was stimulated again with urine. Urine, in the presence of DIDS, induced an inward current with a peak amplitude of −32 pA. Although this particular VSN showed a lack of desensitization to urine in the presence of DIDS, most other VSNs showed desensitizing responses to urine, even when DIDS was present. After a 2-min wash, the urine response recovered to −106 pA. Similar inhibitions were found in the presence of niflumic acid (Fig. 2, B and D). Due to the wide range for peak amplitude of urine-induced inward current across a tested group of VSNs, we normalized the urine response for each cell to that observed in Ringer's. As shown in Fig. 2 (C and D), the amplitude of

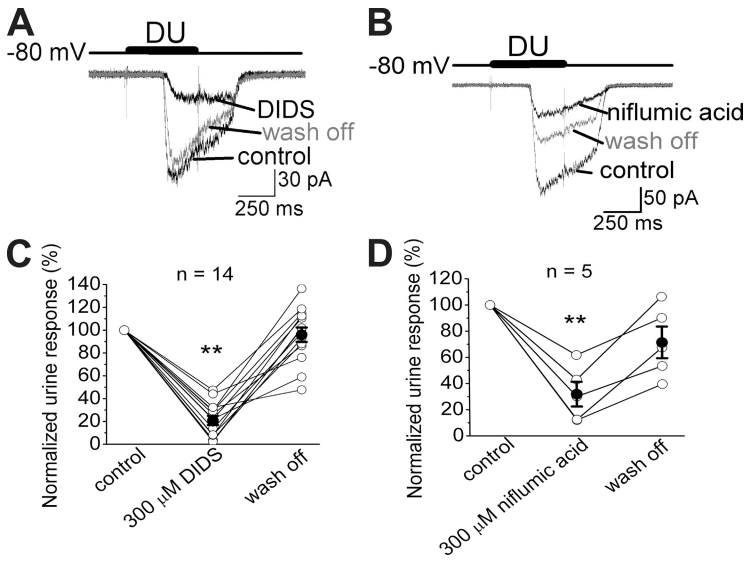

Figure 2. Chloride current in urine-induced responses in isolated mouse VSNs. (A) Urine-induced inward currents decreased in the presence 300 µM of extracellular DIDS. The response recovered after DIDS was washed off. The cell was held at −80 mV and recorded with perforated patch clamp. The interval between urine applications was 2–3 min. (B) 300 µM niflumic acid, another chloride channel blocker, had a similar effect on urine-induced currents as DIDS. The response only partially recovered after niflumic acid was washed off. (C and D) In all the cells tested, DIDS and niflumic acid significantly inhibited the urine-induced inward current, suggesting the involvement of a chloride current in the response. The open circle is the value of the urine response normalized to the initial urine response in Ringer's (control) for each cell. The filled circles and error bars are the mean and SEM for the cells tested in the same conditions. The number of cells is listed on the top of each graph. **, $P < 0.01$, determined with repeated measures one-way ANOVA with Bonferroni test (C) and Friedman with Dunn test (D). DU, 1:500 dilute urine.

the urine-induced inward currents significantly decreased in the presence of DIDS or niflumic acid from that in Ringer's. The urine response in DIDS was 20.9 ± 4.0% (n = 14) of that in Ringer's ($t(41) = 46.7$; $P < 0.01$, repeated measures one-way ANOVA with Bonferroni test; n = 14); the urine response in niflumic acid was 31.9 ± 9.5% of that in Ringer's ($P < 0.05$, Friedman with Dunn test; n = 5). After wash, the responses recovered completely from DIDS (96.0 ± 6.3%; $t(41) = 5.0$; $P > 0.05$, repeated measures one-way ANOVA with Bonferroni test; n = 14), but did not recover fully from the treatment with niflumic acid (71.4 ± 12.1%). Therefore DIDS was used as the chloride channel blocker in the rest of the experiments. The chloride channel blockers inhibited most of the urine-induced current. This suggests that chloride ions carry a large portion of the response.

Because DIDS and niflumic acid can have nonspecific effects (Gribkoff et al., 1996; Becq et al., 1997; Cheng and Sanguinetti, 2009), we confirmed the involvement of chloride current in urine responses by whole cell recordings. We used CsCl in the intracellular solution to eliminate potassium current. To determine how much of the interior of the cell was perfused, we added Lucifer yellow in the intracellular solution and measured the time necessary before we saw fluorescence in the knob. This took ∼2 min. Therefore, we waited at least 2 min after establishing the whole cell configuration before stimulating the cells. To measure the response, we took the peak responses to urine in Ringer's measured at +60 mV and used this time point as our measurement for the rest of the recordings (see dashed line in Fig. 3, A and B). As shown in Fig. 3 (A and B), the reversal potential of the urine response for these two representative cells in Ringer's was close to 0. Overall, the reversal potential for the urine response in Ringer's was 0.4 ± 2.5 mV (mean ± SEM; n = 12). This was similar to the equilibrium potential for Cl^- (E_{Cl}− = −1.9 mV) and the reversal potential of TRPC2 channel (∼0 mV) (Lucas et al., 2003), but much more negative than the equilibrium potential for Na^+ and Ca^{2+} (>+100 mV). To test our hypothesis that chloride ions contribute to the urine response, for each cell we lowered the extracellular Cl^- and tested if the reversal potential for the urine response changed. When $[Cl^-]_o$ was decreased from 151 to 40 mM (E_{Cl}− increased from −1.9 to 32 mV), the reversal potential shifted from 3 to 32 mV (Fig. 3, A and C). This positive shift was consistently observed in all of the

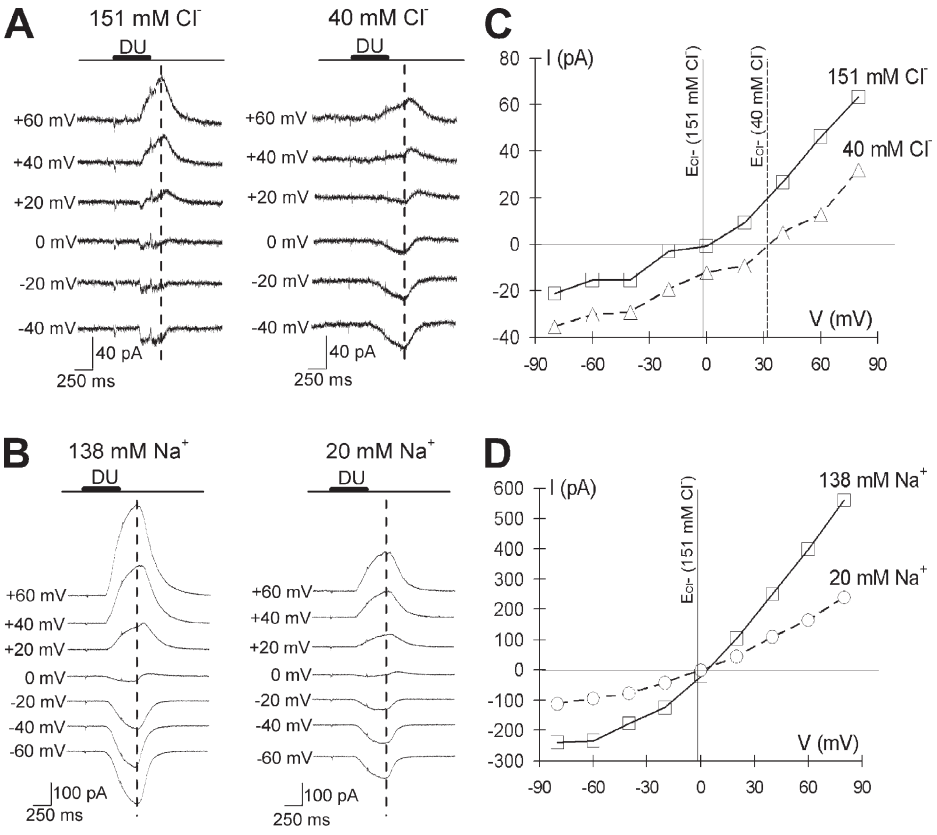

Figure 3. Urine-induced currents shifted reversal potential with changes in extracellular Cl^-, but not with changes in extracellular Na^+. (A) In a representative VSN, changes in extracellular $[Cl^-]$ altered the current response pattern measured by whole cell patch clamp. Ringer's, $[Cl^-]$ = 151 mM; low Cl^- Ringer's with chloride replaced by gluconate, $[Cl^-]$ = 40 mM. (B) Using whole cell patch clamp, the urine response for a VSN was recorded in Ringer's ($[Na^+]$ = 138 mM) and low Na^+ Ringer's with sodium replaced by choline ($[Na^+]$ = 20 mM) at voltage steps from −80 to +80 mV (20-mV increments). (C and D) The I-V at the dashed line in A and B. Currents were measured by subtracting the baseline before urine was applied with that measured at the dashed line. The reversal potential for urine stimulation did not change when extracellular sodium concentration was decreased, but had a positive shift when extracellular chloride concentration was decreased. Potassium currents were blocked by Cs^+ in the pipette solution. Whole cell patch clamp pipette solution contained (in mM): 140 CsCl, 10 HEPES, 5 EGTA, 1 ATP, and 0.5 GTP, pH 7.4, and 285 mmol/kg (glucose). DU, 1:500 dilute urine.

VSNs responding to urine (positive shift: 28 ± 2.0 mV; $n = 8$). To compare the Cl^- and Na^+ contributions to the urine response, we also lowered the extracellular Na^+. As shown in Fig. 3 (B and D), when $[Na^+]_o$ was decreased from 138 to 20 mM, there was no significant change in reversal potential for the urine response (reversal potential of urine response in Ringer's vs. low Na Ringer's: 2.83 ± 0.93 mV vs. 2.00 ± 0.58 mV; $t(2) = 0.56$; $P = 0.630$; paired t test; $n = 3$). Thus, it appeared that chloride current was a large part of the urine-induced currents in VSNs.

Calcium dependence of the chloride currents in mouse VSNs

If the chloride current in urine responses of VSNs is similar to that in odor responses of OSNs, it might be dependent on Ca^{2+} (Hartzell et al., 2005). To test for calcium dependence of the chloride current, we examined the urine-induced inward current in 0 Ca^{2+} Ringer's (with $[Ca^{2+}] << 10$ nM) in the absence and presence of DIDS. As shown in Fig. 4 (A and B), the urine response in 0 Ca^{2+} Ringer's (56.7 ± 9.5%) was decreased from that observed in Ringer's. Adding the chloride channel blocker DIDS (60.3 ± 10.7%) did not alter the magnitude of the urine-induced current compared with that in 0 Ca^{2+} Ringer's (0 Ca^{2+} plus DIDS vs. 0 Ca^{2+}: $P = 0.62$; Wilcoxon signed rank test; $n = 6$). The response to urine was completely eliminated when both extracellular Ca^{2+} and Na^+ were removed (Fig. 4). Thus, the only ion carrying the urine-induced current in 0 Ca^{2+} Ringer's was Na^+. This also eliminated the possibility of activating chloride channels by releasing Ca^{2+} from intracellular stores. Collectively, our recordings in DIDS, 0 Ca^{2+}, 0 Ca^{2+} with DIDS, and 0 Ca^{2+}-0 Na^+ Ringer's support the hypothesis that a Ca^{2+}-activated Cl^- current amplifies the urine-generated response, and that the source of the Ca^{2+} is from the extracellular solution.

Ca^{2+}-activated Cl^- channels were present in VSNs

These results suggest that the Ca^{2+}-activated Cl^- current is the main one contributing to the urine response. To confirm the presence of Ca^{2+}-activated Cl^- channels in VSNs, we recorded the channel activity from inside-out patches on membrane from the dendritic ends with various bath $[Ca^{2+}]$. To exclude the influence of Ca^{2+}-dependent cation channels in VSNs (Liman, 2003; Spehr et al., 2009), we used choline to replace all the cations in the electrode as well as the bath. Thus, chloride ions were the only permeable ions. As shown in Fig. 5, channels with a small conductance opened when bath $[Ca^{2+}]$ increased from 150 nM to 1 mM. This supported the existence of a Ca^{2+}-activated Cl^- channel in VSNs. Among the known channel families for small-conductance Ca^{2+}-activated Cl^- channels that could be mediating these urine responses are the Best family (<6 pS) and two recently reported small-conductance channels, Ano1 (8.3 pS) and Ano2 (0.7–1.3 pS) (Hartzell et al., 2005; Pifferi et al., 2006; Suzuki et al., 2006; Yang et al., 2008; Stephan et al., 2009). Thus, we tested the gene expression of the Best family, Ano1, and Ano2 in VNOs. As shown in Fig. 5 C, *Best2*, *Best3*, *Ano1*, and *Ano2* were expressed in VNOs. The negative controls without RT did not detect any products. Therefore, any or all of these channels could be involved in the urine-induced response. Moreover, because more than one type of Ca^{2+}-acitvated Cl^- channel could be present in each inside-out patch, we presented the average current induced by Ca^{2+} instead of an I-V plot. As shown in Fig. 5 A, at +80 mV, the average current with bath $[Ca^{2+}]$ at 150 nM was 0.02 ± 0.01 pA ($n = 4$). When bath $[Ca^{2+}]$ was increased to 1 mM, the average current increased to 0.33 ± 0.04 pA ($P < 0.01$, paired t test; $n = 4$). Overall, these data from inside-out patches and RT-PCR identified the presence of Ca^{2+}-activated Cl^- channels in VSNs' dendritic tips.

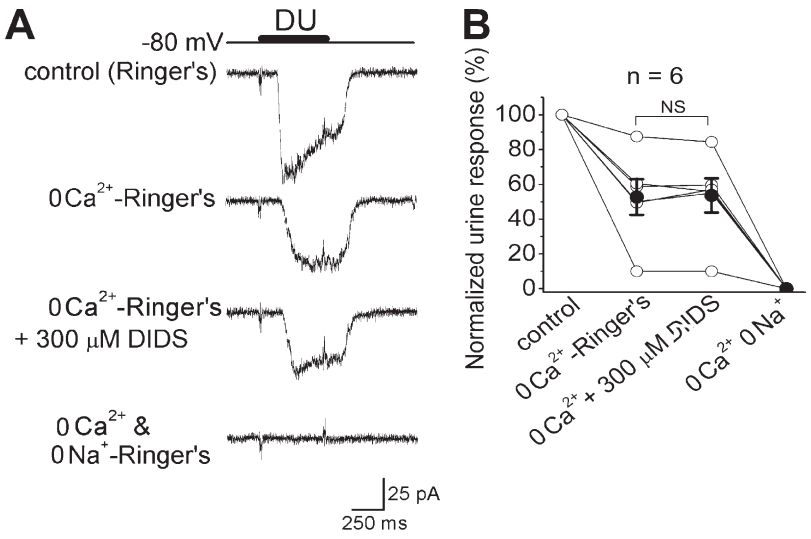

Figure 4. The chloride current in urine responses was dependent of a calcium influx. (A) In a representative VSN recorded using perforated patch clamp technique, the urine-induced inward current ($V_{hold} = -80$ mV) in 0 Ca^{2+} Ringer's ($[Ca^{2+}] << 10$ nM) was not influenced by 300 μM DIDS (second vs. third traces) but eliminated by replacing extracellular Na^+ with choline (0 Ca^{2+}-0 Na^+ Ringer's; bottom trace). The interval between urine applications was 2–3 min. (B) In all the VSNs tested, the amplitude of urine-induced inward current in 0 Ca^{2+} Ringer's was the same as that in 0 Ca^{2+} Ringer's plus 300 μM DIDS. The urine response was abolished in 0 Ca^{2+}-0 Na^+ Ringer's. The open circle is the value of the urine response normalized to the initial urine response in Ringer's (control) for each cell. The filled circles and error bars are the mean and SEM for the cells tested in the same conditions. The number of cells is listed on the top. NS, not significant difference, Wilcoxon signed rank test. DU, 1:500 dilute urine.

NKCC1 contributed to the accumulation of chloride in VSNs

The major contribution of chloride ions to the urine-induced inward current (V_{hold} = −80 mV) as determined by perforated and whole cell recordings suggests that E_{Cl}− in native VSNs is positive to the resting membrane potential, implying a high intracellular chloride, $[Cl^-]_i$, in these cells. We hypothesized that VSNs must have a mechanism to accumulate intracellular Cl^-. NKCC1, an NKCC, is often involved in the regulation of chloride homeostasis in many types of neurons including OSNs and plays an important role in mediating functional development of $GABA_{(A)}$ receptors in the central nervous system (Chen and Sun, 2005; Price et al., 2005). Therefore, we decided to determine if NKCC1 contributed to chloride regulation in VSNs. Three sets of experiments were performed to test the expression and function of NKCC1 in VSNs. First, RT-PCR was used to examine the expression of NKCC1 transcript in VNOs. As shown in Fig. 6 A, NKCC1 mRNA transcript was expressed in VNOs as well as the MOE, which was confirmed by sequencing. Next, we tested for the expression of NKCC1 in coronal VNO slices by immunocytochemistry. It appeared that all of the cells in the VNO, including supporting cells and VSNs, were labeled with a specific anti-NKCC1 antibody (unpublished data). To obtain a better view for the localization of NKCC1 in VSNs, we performed immunocytochemistry on isolated VSNs. We found that NKCC1 was uniformly distributed in VSNs (Fig. 6 B). As a control, the same treatment used for the experimental cells was used for the control cells, except the anti-NKCC1 antibody was left out.

In the last set of experiments, we tested for the function of NKCC1 in isolated VSNs using perforated patch clamp. Urine responses were recorded in the absence and presence of a specific NKCC inhibitor, 10 µM bumetanide. Urine responses were recorded in Ringer's, after a 3-min treatment with bumetanide, and after washing off bumetanide. In the nine cells tested, urine responses in bumetanide (53.3 ± 6.3%) were significantly reduced from those in Ringer's ($t(26) = 4.31$; $P < 0.05$, repeated measures one-way ANOVA with Bonferroni test; $n = 9$). After bumetanide was washed off with Ringer's, urine responses were recovered (93.3 ± 3.1%; $t(26) = 0.56$; $P > 0.05$, repeated measures one-way ANOVA with Bonferroni test; $n = 9$). Because bumetanide

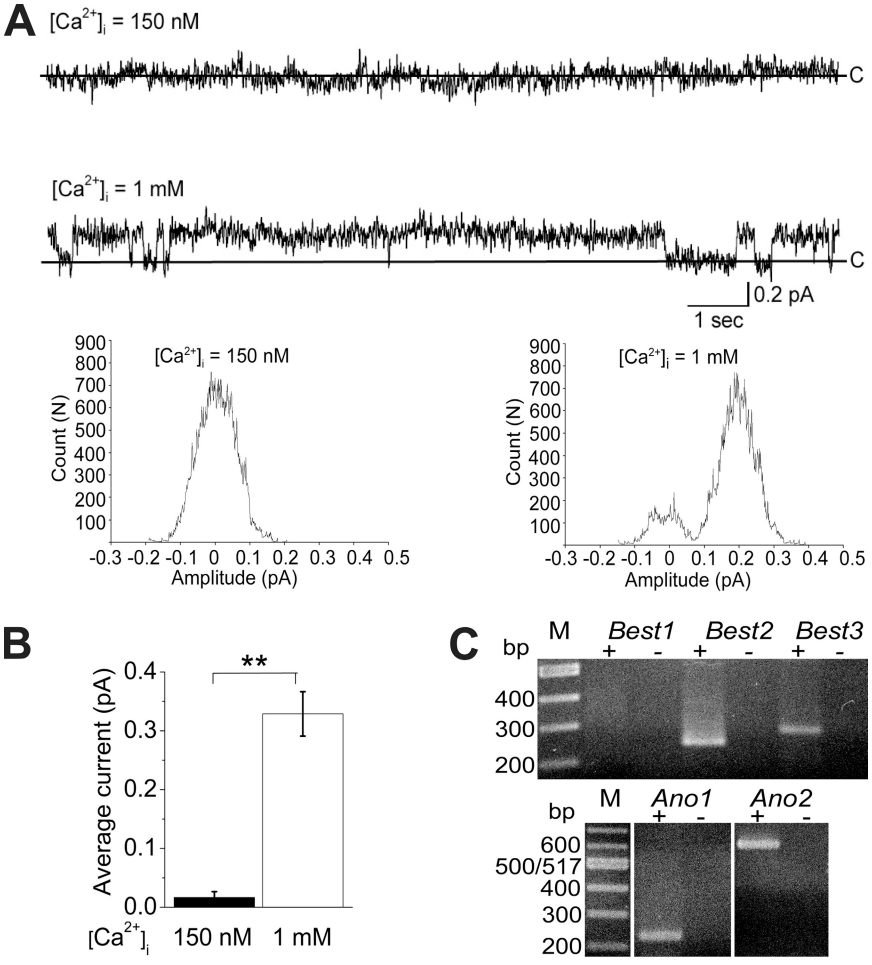

Figure 5. Ca^{2+}-activeted Cl^- channels were present in mouse VSNs. (A) Ca^{2+}-activated Cl^- channels were recorded from inside-out patches taken from the dendritic tips. Channel activity was recorded in a symmetric solution that contained (in mM): 140 choline-Cl, 10 HEPES, and 1 EGTA, pH 7.4, and 285 mmol/kg (glucose). At +80 mV, little channel activity was observed with low intracellular Ca^{2+} concentration (150 nM; top trace), but channel activity greatly increased with 1 mM of intracellular Ca^{2+} added to the bath (bottom trace). C, close state. (B) The average current induced by intracellular calcium at V_{hold} = +80 mV. **, $P < 0.01$, paired *t* test; $n = 4$. (C) RT-PCR experiments detected message from *Best2* (241 bp), *Best3* (280 bp), *Ano1* (226 bp), and *Ano2* (607 bp) in mouse VNO. +, experimental groups; −, control groups without RT.

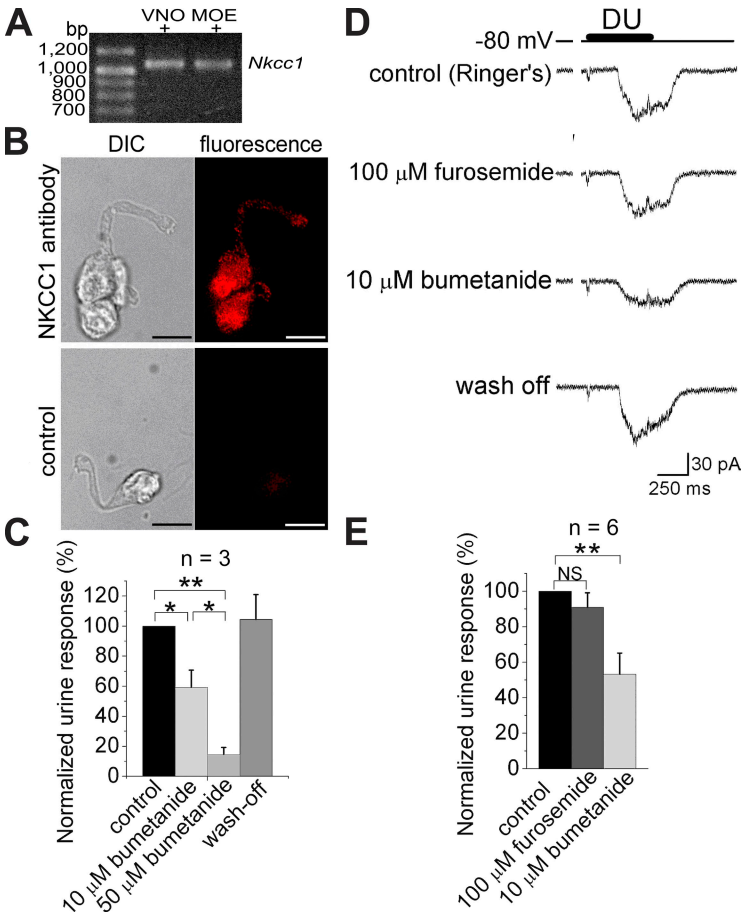

Figure 6. The chloride homeostasis in mouse VSNs was regulated by NKCC1, but not KCC. (A and B) The expression of transcript and protein for NKCC1 using RT-PCR and immunocytochemistry. (C) The dose dependence of an NKCC inhibitor, bumetanide, on the urine response. At 10 μM, bumetanide blocked ∼40% of the urine response, whereas at 50 μM, bumetanide blocked ∼85% of the response (n = 3). (D) In a representative VSN, urine responses were recorded before and after a 5-min incubation of 100 μM furosemide (KCC inhibitor) and 10 μM bumetanide. Furosemide did not influence the urine response, whereas bumetanide decreased about half of the amplitude for the urine response. The response recovered after the blockers were washed off. (E) In all six cells tested, urine-induced inward currents were not influenced by furosemide but decreased ∼50% in the presence of 10 μM bumetanide. **, P < 0.01; *, P < 0.05; NS, not significant difference, as determined with repeated measures one-way ANOVA with Bonferroni test. DU, 1:500 dilute urine.

did not decrease urine responses as much as the chloride channel blockers did, we tested with a higher concentration of bumetanide to determine if 10 μM elicited a maximum effect. After we recorded the urine response in 10 μM bumetanide, we incubated the VSNs in 50 μM bumetanide for 3 min and recorded the urine response. Urine responses in 50 μM bumetanide (14.5 ± 4.7%) were significantly smaller than those in 10 μM bumetanide (59.2 ± 11.5%; $t(8) = 4.86$; $P < 0.05$, repeated measures one-way ANOVA with Bonferroni test; $n = 3$; Fig. 6 C). Urine responses recovered after bumetanide was washed off with Ringer's. Bumetanide at concentrations higher than 100 μM has been reported to inhibit KCCs, which maintain a low intracellular chloride level (Aull, 1981). If 50 μM bumetanide inhibited KCC, we would have expected to observe a smaller inhibition of urine responses than with 10 μM bumetanide because 50 μM bumetanide would have been altering both the influx and the efflux of Cl^-. However, 50 μM bumetanide had a stronger inhibition on urine responses than 10 μM. Therefore, it appears that 50 μM bumetanide only inhibited NKCC and not any KCC. To further confirm this, we used the KCC blocker, 100 μM furosemide, to determine its influence on urine responses. We compared urine responses in Ringer's and after a 5-min treatment with furosemide. If any KCC (KCC1-4) played a role in regulating $[Cl^-]_i$ in VSNs, the inhibition of these transporters would have resulted in an increased $[Cl^-]_i$ and increased urine responses. However, as shown in Fig. 6 (D and E), the urine response in 100 μM furosemide (91.0 ± 8.0%; $n = 6$) was not statistically different from the response in Ringer's ($t(17) = 0.3239$; $P > 0.05$, repeated measures one-way ANOVA with Bonferroni test; $n = 6$). As a control, the same cells were also tested in 10 μM bumetanide. After furosemide was washed off, the cells were incubated in bumetanide for 5 min and tested with urine. Urine responses in 10 μM bumetanide (53.2 ± 11.9%) were significantly decreased ($t(17) = 3.14$; $P < 0.05$, repeated measures one-way ANOVA with Bonferroni test; $n = 6$). These data suggest that NKCC1 is important in maintaining a high $[Cl^-]_i$, while it is likely that KCC does not play any functional role in VSNs. Again, none of these inhibitors alone induced any response in VSNs, as there was no change on the baseline current ($V_{hold} = -80$ mV) when VSNs were incubated in inhibitors.

DISCUSSION

Our results suggest that the urine-responsive VSNs maintain high $[Cl^-]_i$ because all of the VSNs we tested showed that a Ca^{2+}-activated Cl^- current carried a large

part of the urine-induced response. We draw this conclusion based on several lines of evidence. First, the reversal potential of the urine response did not change when $[Na^+]_o$ decreased, but was shifted positively when $[Cl^-]_o$ decreased. Second, two chloride channels blockers, DIDS and niflumic acid, blocked an average of 80% of the urine-induced inward current. DIDS had no influence on the urine response when bath Ca^{2+} was 0, suggesting that an influx of Ca^{2+} was necessary to activate the chloride current. Third, the removal of extracellular Ca^{2+} and Na^+ eliminated the current induced by urine stimulation. Fourth, NKCC1, a Cl^- cotransporter that moves chloride into the cells, is expressed in VSNs, and its blocker, 50 µM bumetanide, decreased the urine-induced inward current ~85%. On the other hand, a KCC blocker, 100 µM furosemide, had no influence on the urine-induced inward current. All these data support the role for a Ca^{2+}-activated Cl^- current in pheromone/odor detection of VSNs.

Ca^{2+}-activated Cl^- channels in VSNs

Several groups have examined the current elicited by urine in VSNs and not observed any chloride current in the response. Lucas et al. (2003) did not report chloride current in urine response by whole cell recordings. There are several possible reasons why they did not see a chloride current. First, they used a different cell isolation procedure from us. Second, they used anesthesia before cell isolation. Third, their isolation was at 37°C. Fourth, they were focused on the initial channel activated in urine responses, and the chloride current is a downstream element of the response. Although Spehr et al. (2009) did inside-out patches to record the Ca^{2+}-dependent channel activity, they did not detect any Ca^{2+}-activated Cl^- channel activity. However, the conductance of chloride channels is quite small compared with cation channels, and it might be too low to be detected in the ramp currents that they measured. Our inside-out patch data of single-channel activity show that there is a Ca^{2+}-activated Cl^- channel in the dendritic tips of VSNs. Under our recording conditions, the only ion that could move across the membrane was Cl^-. The conductance of this chloride channel appears to be very small (<3 pS).

Best2 was first suggested as the Ca^{2+}-activated Cl^- channel mediating odor detection in mouse OSNs, so it seemed reasonable to see if it is involved in the odor response in VSNs (Pifferi et al., 2006). We tested for the expression of Best2 by RT-PCR and immunocytochemistry and found that Best2 was localized on the dendritic membrane (unpublished data). These results are similar to those of Klimmeck et al. (2009), where they also showed the presence of Best2 on the dendrites of a subset of VSNs (Klimmeck et al., 2009). However, there are other possible candidates for the low conductance Ca^{2+}-activated Cl^- channels that amplify the odor response. We tested for them with RT-PCR and found that *Best3*, *Ano1*, and *Ano2* were also expressed in VNO. Thus, any or all of these chloride channels could be amplifying the urine responses in VSNs.

Ca^{2+} influx is necessary to activate the Ca^{2+}-activated Cl^- channels

In our study, when we removed the extracellular Ca^{2+}, we observed a 45% decrease in urine-induced inward current (Fig. 4). This decrease is not as large as that observed in the presence of the chloride channel blocker, DIDS (80%). This was an unexpected result because it appears that the chloride current was dependent on a Ca^{2+} influx, so we expected to see an 80% or more decrease in the urine responses in 0 Ca^{2+} Ringer's compared with that in Ringer's. One possible explanation for our results is that Ca^{2+} partially blocks the TRPC2 channels in a manner similar to the Ca^{2+} block of the CNG channels in OSNs (Zufall and Firestein, 1993). If this is true, blocking the chloride channels with DIDS should have no effect on the urine responses in 0 Ca^{2+} Ringer's. Indeed, there was no difference in the urine response in 0 Ca^{2+} Ringer's and 0 Ca^{2+} Ringer's plus DIDS (Fig. 4). This was confirmed by removing bath Na^+ (0 Ca^{2+}-0 Na^+ Ringer's) and completely eliminating the urine-induced current. Thus, Ca^{2+} influx is necessary to activate the Ca^{2+}-activated Cl^- channels.

Biological significance of Ca^{2+}-activated Cl^- currents in VSNs

Our data support the idea that chloride ions carry most of the current elicited by odorants/pheromones. The chloride current is a downstream element to the initial cation influx and greatly amplifies the initial signal. For this chloride amplification to occur, under normal physiological conditions, the microvilli of VSNs must be exposed to extracellular Ca^{2+}. Although the lumen of VNO is filled with fluid from vomeronasal glands (Keverne, 1999), very little is known about its ionic composition. If we assume that the ionic composition of the VNO luminal fluid is similar to that in the mucus of MOE, there would be divalent cations present (Joshi et al., 1987; Chiu et al., 1989). The presence of extracellular Ca^{2+} would be sufficient to allow the signaling cascade to occur in the presence of odorants/pheromones because $[Cl^-]_i$ is high and will efflux when the chloride channels are open.

One consideration is what the $[Cl^-]_o$ under normal physiological conditions is. If extracellular Cl^- is low, this will increase the driving force for Cl^- to leave the cell. On the other hand, if extracellular Cl^- is high, the driving force for Cl^- to leave the cell is lessened. Under our normal recording conditions, extracellular Cl^- is 151 mM, similar to interstitial fluid (Reuter et al., 1998). Thus, although it is possible that VNO luminal fluid has higher levels of Cl^- than our normal recording conditions, it seems unlikely.

In summary, we have elucidated a new mechanism in mouse VSNs by which the urine responses are amplified by a Ca^{2+}-activated Cl^- current. This amplification could increase the sensitivity of VSNs to pheromones/odors. Further, chloride ions carry the majority of currents elicited in response to odors. The ability to maintain high intracellular Cl^- would be important for these sensory neurons to effectively detect chemicals as long as calcium ions are in the environment.

We thank Travis Verret, Carol Taylor-Burds, Dr. Janet Woodcock-Mitchell, and Dr. Eugene Delay for their critical reading of the manuscript. We also thank Dr. Judith Van Houten for her help with RT-PCR experiments.

This work was supported by National Institutes of Health grants NIH-DC006939 and NIH-P20RR16435.

Edward N. Pugh Jr. served as editor.

Submitted: 29 May 2009
Accepted: 2 December 2009

REFERENCES

Aull, F. 1981. Potassium chloride cotransport in steady-state ascites tumor cells. Does bumetanide inhibit? *Biochim. Biophys. Acta.* 643:339–345. doi:10.1016/0005-2736(81)90079-1

Becq, F., Y. Hamon, A. Bajetto, M. Gola, B. Verrier, and G. Chimini. 1997. ABC1, an ATP binding cassette transporter required for phagocytosis of apoptotic cells, generates a regulated anion flux after expression in Xenopus laevis oocytes. *J. Biol. Chem.* 272:2695–2699. doi:10.1074/jbc.272.5.2695

Breer, H., J. Fleischer, and J. Strotmann. 2006. The sense of smell: multiple olfactory subsystems. *Cell. Mol. Life Sci.* 63:1465–1475. doi:10.1007/s00018-006-6108-5

Chen, H., and D. Sun. 2005. The role of Na-K-Cl co-transporter in cerebral ischemia. *Neurol. Res.* 27:280–286. doi:10.1179/016164105X25243

Cheng, L., and M.C. Sanguinetti. 2009. Niflumic acid alters gating of HCN2 pacemaker channels by interaction with the outer region of S4 voltage sensing domains. *Mol. Pharmacol.* 75:1210–1221. doi:10.1124/mol.108.054437

Chiu, D., T. Nakamura, and G.H. Gold. 1989. Ionic composition of toad olfactory mucus measured with ion selective microelectrodes. *Chem. Senses.* 13:677–678.

Døving, K.B., and D. Trotier. 1998. Structure and function of the vomeronasal organ. *J. Exp. Biol.* 201:2913–2925.

Gribkoff, V.K., J.T. Lum-Ragan, C.G. Boissard, D.J. Post-Munson, N.A. Meanwell, J.E. Starrett Jr., E.S. Kozlowski, J.L. Romine, J.T. Trojnacki, M.C. Mckay, et al. 1996. Effects of channel modulators on cloned large-conductance calcium-activated potassium channels. *Mol. Pharmacol.* 50:206–217.

Hartzell, C., I. Putzier, and J. Arreola. 2005. Calcium-activated chloride channels. *Annu. Rev. Physiol.* 67:719–758. doi:10.1146/annurev.physiol.67.032003.154341

Joshi, H., M.L. Getchell, B. Zielinski, and T.V. Getchell. 1987. Spectrophotometric determination of cation concentrations in olfactory mucus. *Neurosci. Lett.* 82:321–326. doi:10.1016/0304-3940(87)90276-X

Keverne, E.B. 1999. The vomeronasal organ. *Science.* 286:716–720. doi:10.1126/science.286.5440.716

Kleene, S.J. 1997. High-gain, low-noise amplification in olfactory transduction. *Biophys. J.* 73:1110–1117. doi:10.1016/S0006-3495(97)78143-8

Kleene, S.J. 2008. The electrochemical basis of odor transduction in vertebrate olfactory cilia. *Chem. Senses.* 33:839–859. doi:10.1093/chemse/bjn048

Klimmeck, D., P.C. Daiber, A. Brühl, A. Baumann, S. Frings, and F. Möhrlen. 2009. Bestrophin 2: an anion channel associated with neurogenesis in chemosensory systems. *J. Comp. Neurol.* 515:585–599. doi:10.1002/cne.22075

Kurahashi, T., and K.W. Yau. 1993. Co-existence of cationic and chloride components in odorant-induced current of vertebrate olfactory receptor cells. *Nature.* 363:71–74. doi:10.1038/363071a0

Liman, E.R. 2003. Regulation by voltage and adenine nucleotides of a Ca2+-activated cation channel from hamster vomeronasal sensory neurons. *J. Physiol.* 548:777–787. doi:10.1113/jphysiol.2002.037119

Lucas, P., K. Ukhanov, T. Leinders-Zufall, and F. Zufall. 2003. A diacylglycerol-gated cation channel in vomeronasal neuron dendrites is impaired in TRPC2 mutant mice: mechanism of pheromone transduction. *Neuron.* 40:551–561. doi:10.1016/S0896-6273(03)00675-5

Nilius, B., and G. Droogmans. 2003. Amazing chloride channels: an overview. *Acta Physiol. Scand.* 177:119–147. doi:10.1046/j.1365-201X.2003.01060.x

Pifferi, S., G. Pascarella, A. Boccaccio, A. Mazzatenta, S. Gustincich, A. Menini, and S. Zucchelli. 2006. Bestrophin-2 is a candidate calcium-activated chloride channel involved in olfactory transduction. *Proc. Natl. Acad. Sci. USA.* 103:12929–12934. doi:10.1073/pnas.0604505103

Price, T.J., F. Cervero, and Y. de Koninck. 2005. Role of cation-chloride-cotransporters (CCC) in pain and hyperalgesia. *Curr. Top. Med. Chem.* 5:547–555. doi:10.2174/1568026054367629

Reuter, D., K. Zierold, W.H. Schröder, and S. Frings. 1998. A depolarizing chloride current contributes to chemoelectrical transduction in olfactory sensory neurons in situ. *J. Neurosci.* 18:6623–6630.

Schild, D., and D. Restrepo. 1998. Transduction mechanisms in vertebrate olfactory receptor cells. *Physiol. Rev.* 78:429–466.

Shimazaki, R., A. Boccaccio, A. Mazzatenta, G. Pinato, M. Migliore, and A. Menini. 2006. Electrophysiological properties and modeling of murine vomeronasal sensory neurons in acute slice preparations. *Chem. Senses.* 31:425–435. doi:10.1093/chemse/bjj047

Spehr, J., S. Hagendorf, J. Weiss, M. Spehr, T. Leinders-Zufall, and F. Zufall. 2009. Ca2+-calmodulin feedback mediates sensory adaptation and inhibits pheromone-sensitive ion channels in the vomeronasal organ. *J. Neurosci.* 29:2125–2135. doi:10.1523/JNEUROSCI.5416-08.2009

Stephan, A.B., E.Y. Shum, S. Hirsh, K.D. Cygnar, J. Reisert, and H. Zhao. 2009. ANO2 is the cilial calcium-activated chloride channel that may mediate olfactory amplification. *Proc. Natl. Acad. Sci. USA.* 106:11776–11781.

Suzuki, M., T. Morita, and T. Iwamoto. 2006. Diversity of Cl(−) channels. *Cell. Mol. Life Sci.* 63:12–24. doi:10.1007/s00018-005-5336-4

Ukhanov, K., T. Leinders-Zufall, and F. Zufall. 2007. Patch-clamp analysis of gene-targeted vomeronasal neurons expressing a defined V1r or V2r receptor: ionic mechanisms underlying persistent firing. *J. Neurophysiol.* 98:2357–2369. doi:10.1152/jn.00642.2007

Yang, Y.D., H. Cho, J.Y. Koo, M.H. Tak, Y. Cho, W.S. Shim, S.P. Park, J. Lee, B. Lee, B.M. Kim, et al. 2008. TMEM16A confers receptor-activated calcium-dependent chloride conductance. *Nature.* 455:1210–1215. doi:10.1038/nature07313

Zhang, P., C. Yang, and R.J. Delay. 2008. Urine stimulation activates BK channels in mouse vomeronasal neurons. *J. Neurophysiol.* 100:1824–1834. doi:10.1152/jn.90555.2008

Zufall, F., and S. Firestein. 1993. Divalent cations block the cyclic nucleotide-gated channel of olfactory receptor neurons. *J. Neurophysiol.* 69:1758–1768.

Zufall, F., and T. Leinders-Zufall. 2007. Mammalian pheromone sensing. *Curr. Opin. Neurobiol.* 17:483–489. doi:10.1016/j.conb.2007.07.012

Zufall, F., S. Firestein, and G.M. Shepherd. 1994. Cyclic nucleotide-gated ion channels and sensory transduction in olfactory receptor neurons. *Annu. Rev. Biophys. Biomol. Struct.* 23:577–607. doi:10.1146/annurev.bb.23.060194.003045

Zufall, F., K.R. Kelliher, and T. Leinders-Zufall. 2002. Pheromone detection by mammalian vomeronasal neurons. *Microsc. Res. Tech.* 58:251–260. doi:10.1002/jemt.10152